

## Di-jet correlation in Au + Au and Cu + Cu collisions from PHENIX

Jiangyong Jia

Columbia University and Nevis Laboratories, Irvington, NY 10533, USA

Received March 19, 2021

**Abstract.** PHENIX has measured the two particle azimuth correlation in Au + Au at  $\sqrt{s} = 200$  GeV. Jet shape and yield at the away side are found to be strongly modified at intermediate and low  $p_T$ , and the modifications vary dramatically with  $p_T$  and centrality. At high  $p_T$ , away side jet peak reappears but the yield is suppressed. Similar jet strength is found for Au + Au and Cu + Cu collisions with similar number of participant nucleons.

*Keywords:* Correlation function, Jet, elliptic flow, Au + Au, Cu + Cu  
*PACS:* 25.75.-q

### 1. Introduction

We summarize the two particle azimuthal correlation results presented in QM2005 poster. Due to space limitation, please refer to [ 1, 2] for the technical details and the results on reaction plane dependence of the jet correlation.

### 2. Jet Correlation at Intermediate $p_T$ in Au + Au

The Au + Au results are obtained from 1 billion minimum bias events. According to [ 2], we parameterized the correlation function  $C(\Delta\phi)$  (CF) as,

$$C(\Delta\phi) = J(\Delta\phi) + \xi (1 + 2v_2^t v_2^a \cos \Delta 2\phi) \quad (1)$$

$J(\Delta\phi)$  represents the contribution from jet.  $v_2^t$  and  $v_2^a$  are the elliptic flow for the trigger and associated particles, respectively.  $\xi$  is the only free normalization factor, which is fixed using the ZYAM assumption [ 3, 4].

A typical correlation function from central Au + Au collisions is shown in Fig.1.  $v_2$  values in the corresponding  $p_T$  selections are about 0.062 in 2.5-4 GeV/c, and 0.041 in 1-2.5 GeV/c ranges. The away side shape is very broad and non-gauss

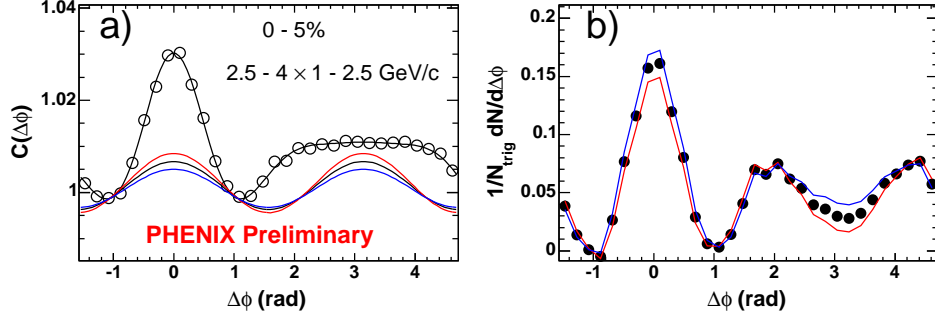


**Fig. 1.** a) Correlation function in 0-5% centrality bin, the lines indicated the level of flow background and the systematic errors. b) Correspondingly background subtracted per-trigger yield.

like. It has a wide plateau that expands to about  $\pi \pm 1$  radian. After the flow contribution (shown by the curves) is subtracted, a dip appears around  $\pi$  as shown in Fig.1b. This shape can not be due to the random walk type of broadening of the jets from energy loss. It is qualitatively consistent with Cherenkov gluons [ 5] or shock wave [ 6] excited by the travelling jets in the medium.

To quantify the modifications of the jet shape, we study the jet yield in three different  $\Delta\phi$  regions: near side jet region ( $|\Delta\phi| < \pi/3$ ), the away side dip region ( $|\Delta\phi - \pi| < \pi/6$ ), and the away side shoulder region ( $|\Delta\phi - \pi \pm \pi/3| < \pi/6$ ). The shoulder region is sensitive to the novel medium effects, while the dip region is sensitive to the punch through jet contribution. Fig.2 plots the jet yields in the three regions as function of  $p_{T,assoc}$  for four centralities. In 0-5% centrality bin, there is a large separation between the yields for the dip region and near side jet region, persistent to large  $p_T$ . In more peripheral collisions, the yield of the dip region becomes closer or even exceeds that for the shoulder region, consistent with the returning of the away side jet to a normal gauss shape.

The modification of the jet shape and yield can be quantified by  $I_{cp}$ , i.e. the ratios of the per-trigger yield between central bin and 60-92% peripheral bin, as shown in Fig.3 for the three  $\Delta\phi$  regions. In 0-5% central bin,  $I_{cp}$  is well above one for the away shoulder region at low  $p_{T,assoc}$ , and decreases toward larger  $p_{T,assoc}$ . This is in sharp contrast with the away dip region, which shows a suppression of the  $I_{cp}$ , although both regions have similar  $p_T$  dependence. We also see a modest enhancement of the per-trigger yield at the near side at low  $p_{T,assoc}$ . This plus the strong suppression in the away side dip region are consistent with STAR's observation in a earlier publication [ 7] (for a somewhat different  $p_T$  selection). Finally,  $I_{cp}$  for all three  $\Delta\phi$  regions approach unity towards peripheral collisions.

### 3. Jet Correlation from Low $p_T$ to High $p_T$ in Au + Au

Jet correlations at different  $p_T$  reflect different aspect of the interaction between jet and the medium. The results are summarized in Fig.4, where we plot the per-trigger yield as function of both  $p_T$  (vertical) and centrality (horizontal). Along the vertical direction, we can see how the away side jet evolves from a cone type of structure at intermediate  $p_T$  to a relatively flat distribution at moderately high  $p_T$ , to a reappeared jet structure at high  $p_T$ . Along the horizontal direction, we can also see that the modifications of the away side jet shape depend strongly on centrality. Further detailed discussions can be found in [ 2].

### 4. Comparison of High $p_T$ $\pi^0 - h$ Correlation Between Au + Au and Cu + Cu

If jet modifications are mainly determined by the size of the medium created in the heavy-ion collisions, we should expect a similar modification in Cu + Cu collisions with similar  $N_{\text{part}}$  as in Au + Au. However, they have very different  $v_2$  systematics due to their totally different shape of the overlap region. Fig.5 shows the comparison of the high  $p_T$   $\pi^0 - h$  correlation functions together with the estimated flow background for 30-40% Au + Au centrality and 0-10% Cu + Cu centrality bin. Both have similar number of participants and number of collisions:  $N_{\text{part}} = 98$  and  $N_{\text{coll}} = 183$  in Cu + Cu and  $N_{\text{part}} = 114$  and  $N_{\text{coll}} = 220$  in Au + Au. The amplitudes of the correlation functions, which reflect the ratio of jet signal to the combinatoric background, are larger in Cu + Cu case because Cu + Cu has a smaller  $N_{\text{part}}$  and  $N_{\text{coll}}$ . However, one see that the background subtracted distributions in both systems are qualitatively similar to each other.

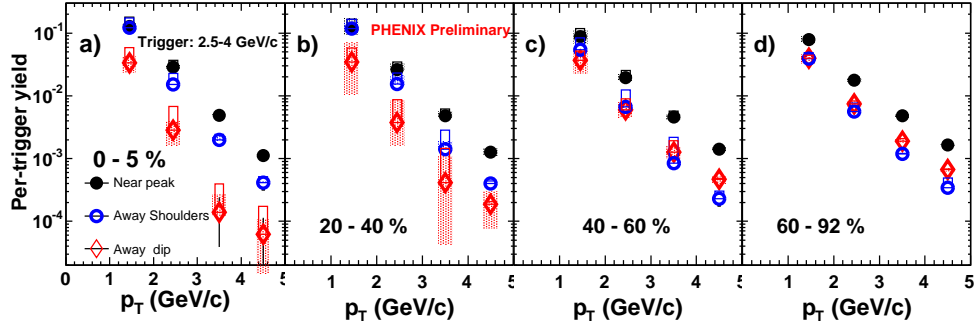


**Fig. 2.** The yield for trigger 2.5-4 GeV/c plotted as function of associated hadron  $p_T$  for four different centrality bins.

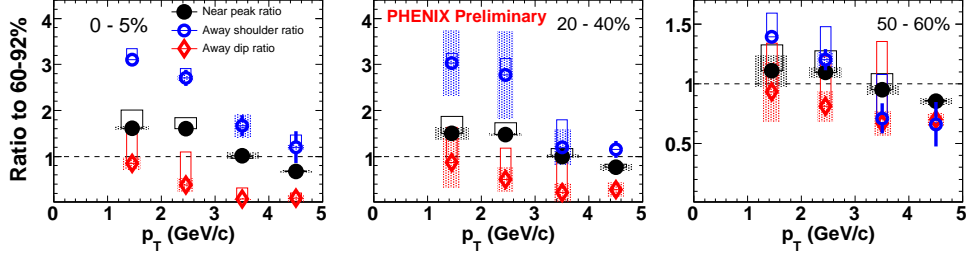


Fig. 3. Ratio of the per-trigger yield between central bin and 60-92% centrality bin ( $I_{CP}$ ) for the three  $\Delta\phi$  ranges

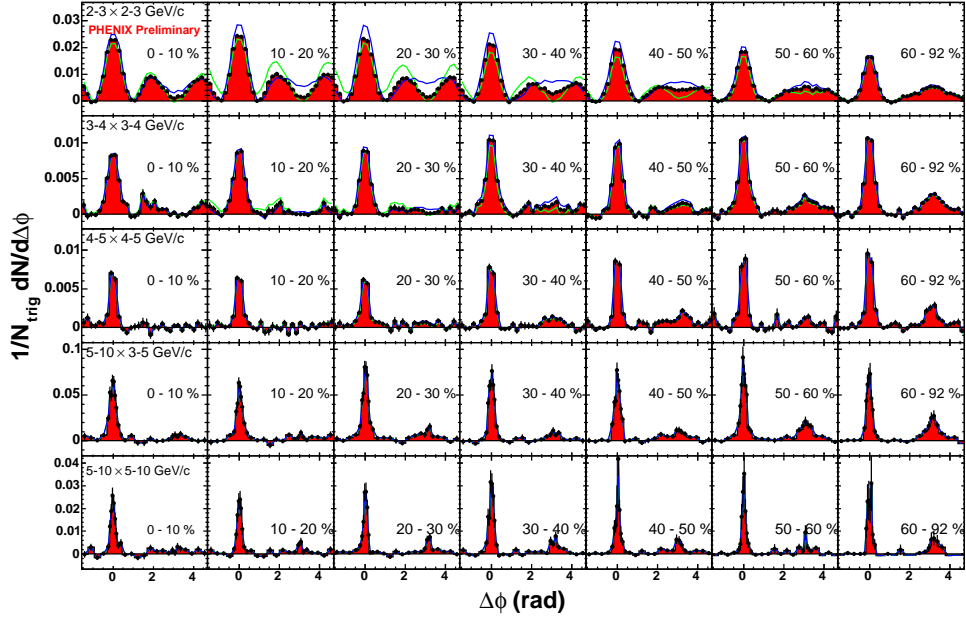
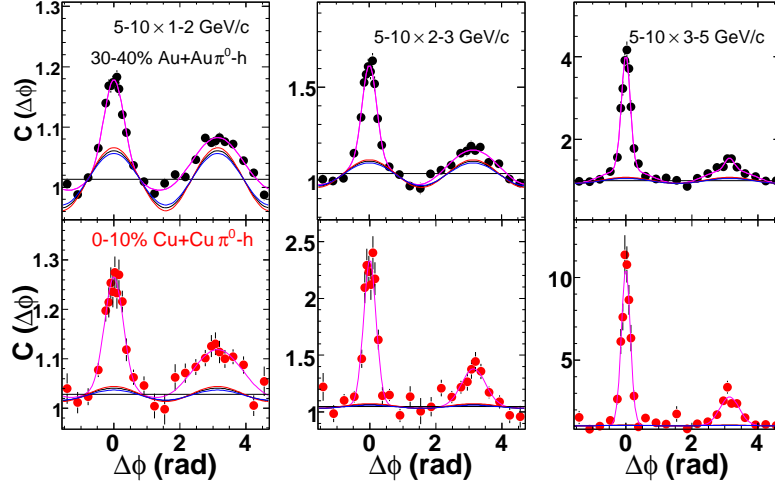


Fig. 4. Background subtracted per-trigger jet yield in  $\Delta\phi$  as function of  $p_T$  (vertical) and centrality (horizontal).

## References

1. N. Grau [PHENIX Collaboration], arXiv:nucl-ex/0511046.
2. J. Jia, arXiv:nucl-ex/0510019.
3. N. N. Ajitanand *et al.*, Phys. Rev. C **72**, 011902 (2005)
4. S. S. Adler *et al.* [PHENIX Collaboration], arXiv:nucl-ex/0507004.
5. I. M. Dremin, JETP Lett. **30** (1979) 140 [Pisma Zh. Eksp. Teor. Fiz. **30**



**Fig. 5.** The  $\pi^0$ -h correlation functions for three different associated charged hadron  $p_T$  ranges (with fixed triggering  $\pi^0$   $p_T$ : 5-10 GeV/c). (Top row) 30-40% most central Au + Au centrality bin, and (Bottom row) 0-10% most central Cu + Cu centrality bin.

- (1979) 152]; V. Koch, A. Majumder and X. N. Wang, arXiv:nucl-th/0507063.  
 6. J. Casalderrey-Solana, E. V. Shuryak and D. Teaney, arXiv:hep-ph/0411315.  
 7. C. Adler *et al.* [STAR Collaboration], Phys. Rev. Lett. **90**, 082302 (2003)